



Production of WZ Events in $p\bar{p}$ Collisions at $\sqrt{s} = 1.96$ TeV and Limits on Anomalous WWZ Couplings

The DØ Collaboration
URL <http://www-d0.fnal.gov>
(Dated: February 4, 2005)

We present a search for WZ production with subsequent decay to $\ell\bar{\ell}'\nu$ (ℓ and $\ell' = e$ or μ) using center-of-mass energy $\sqrt{s} = 1.96$ TeV $p\bar{p}$ collision data. The data was collected by the DØ experiment during 2002-2004 at the Fermilab Tevatron. Three events with WZ decay characteristics are observed. With an estimated background of 0.71 ± 0.08 events and integrated luminosities ranging from 285 - 320 pb^{-1} for different trilepton final states, we measure the WZ production cross section to be $4.5^{+3.8}_{-2.6}$ pb, and set a 95% C.L. upper limit of 13.3 pb for this quantity. The 95% C.L. limits for anomalous couplings corresponding to a form factor scale $\Lambda = 1$ TeV are found to be $-0.53 < \lambda_Z < 0.56$, $-0.57 < \Delta g_1^Z < 0.76$ and $-2.0 < \Delta \kappa_Z < 2.4$. For $\Lambda = 1.5$ TeV, the corresponding limits are $-0.48 < \lambda_Z < 0.48$ and $-0.49 < \Delta g_1^Z < 0.66$.

The $SU(2)_L \times U(1)_Y$ structure of the standard model (SM) implies that the electroweak gauge bosons W and Z can interact with one another through trilinear and quartic gauge-boson vertices. For SM $p\bar{p}$ interactions, the WZ production cross section σ_{WZ} depends, in particular, on the WWZ gauge coupling shown in Fig. 1. More generally, WWZ interactions can be described by an effective Lagrangian with arbitrary parameters g_1^Z , λ_Z and κ_Z [1]. In the SM, $g_1^Z = \kappa_Z = 1$ and $\lambda_Z = 0$. Non-SM values of these couplings may increase σ_{WZ} significantly. Therefore a measurement of this quantity provides a sensitive test of the strength of the WWZ interaction. This test probes for low energy remnants of new physics operating at a higher scale that complements searches to be carried out with accelerators that produce collisions at higher energy.

A test for anomalous trilinear boson couplings using σ_{WZ} is unique in that WZ diagrams contain only WWZ , and not $WW\gamma$, vertices. Anomalous trilinear gauge boson coupling limits produced using characteristics of W^+W^- production [2–4] are sensitive to both and must make an assumption about the relating the $WW\gamma$ couplings to the WWZ couplings. See, for instance, the HISZ [5] relations. Furthermore, as this analysis is performed using event candidates ($W^\pm Z$) that are unavailable in e^+e^- colliders [3], it provides a unique measurement of WWZ anomalous coupling limits.

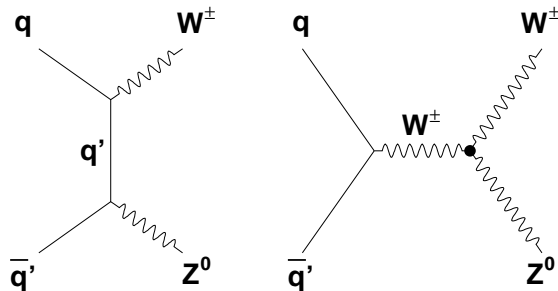


FIG. 1: Tree-level diagrams for WZ production in $p\bar{p}$ collisions. The diagram on the right contains the WWZ trilinear gauge coupling vertex.

In Run I of Fermilab’s Tevatron, DØ established that $\sigma_{WZ} < 47$ pb at 95% C.L. From this, DØ set the 95% C.L. limits $|g_1^Z - 1| < 1.63$ and $|\lambda_Z| < 1.42$ for a form factor scale $\Lambda = 1$ TeV [2]. With a higher center-of-mass energy of $\sqrt{s} = 1.96$ TeV producing a 20% higher cross section ($\sigma_{WZ} = 3.7 \pm 0.1$ pb [6]), more luminosity, and an improved detectors, the Run II Tevatron program opens a new window for studies of WZ diboson production. The CDF Collaboration recently published a 15.2 pb upper limit at 95% C.L. on the combined cross section for WZ and ZZ at $\sqrt{s} = 1.96$ TeV [7].

The cleanest WZ signals consist of final states with three charged leptons (trileptons) and a neutrino that emerge from coinciding leptonic decays of the Z and the W . Requiring three isolated high transverse momentum (p_T) leptons and large missing transverse energy (\cancel{E}_T) associated with the neutrino, strongly suppresses all known SM backgrounds. However, product branching ratios are only 1.5% for trilepton final states ($e\bar{e}\mu$, $\mu\bar{\mu}e$, eee and $\mu\mu\mu$).

The DØ detector comprises several sub-detectors, and a trigger and data acquisition system [8]. The central-tracking system consists of a silicon micro-strip tracker (SMT) and a central fiber tracker (CFT) located within a 2 T superconducting solenoid magnet [9]. The SMT has $\approx 800,000$ individual strips with excellent coverage up to pseudo-rapidity $|\eta| < 3$. The CFT contains eight thin coaxial barrels, each supporting two doublets of overlapping scintillating fibers of 0.835 mm diameter. One doublet is oriented parallel to the collision axis, and the other tilted with respect to the axis by $\pm 3^\circ$ stereo angles that alternate with layer. CFT signals travel via clear light fibers to solid-state photon counters (VLPC) that have $\approx 80\%$ quantum efficiency.

Central and forward preshower detectors located just outside of the superconducting coil and in front of the calorimetry are constructed of several layers of extruded triangular scintillator strips that are read out using wavelength-shifting fibers and VLPCs. Beyond the preshower detectors are three uranium/liquid-argon calorimeters, each housed in a separate cryostat [8]: a central section (CC) covering $|\eta| \leq 1.1$ and two end calorimeters (EC) extending coverage to $|\eta| \leq 4.2$. In addition to the preshower detectors, scintillators between the CC and EC cryostats provide sampling of developing showers for $1.1 < |\eta| < 1.4$. Luminosity is measured using plastic scintillator arrays located in front of the EC cryostats and covering $2.7 < |\eta| < 4.4$.

A muon system [9] resides beyond the calorimetry, and consists of a layer of tracking detectors and scintillation trigger counters before 1.8 T toroidal magnets, followed by two more similar layers after the toroids. Muon tracking for $|\eta| < 1$ relies on 10 cm wide drift tubes [8], while 1 cm mini-drift tubes are used for $1 < |\eta| < 2$.

Trigger and data acquisition systems are designed to accommodate high luminosities of the upgraded Fermilab Tevatron in Run II. Based on preliminary information from tracking, calorimetry, and muon systems, the output of

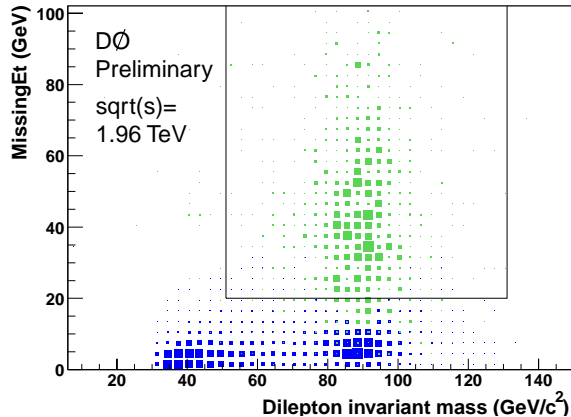


FIG. 2: Dilepton invariant mass vs. \cancel{E}_T distribution for expected $WZ \rightarrow \mu\mu\mu\nu$ events (green or light grey) and for expected $Z + \text{jet}$ background events (blue or dark grey). The central box shows the event selection criteria.

the first level of the trigger is used to limit the rate for accepted events to ≈ 1.5 kHz. With more refined information at the second level, the rate is reduced further to ≈ 800 Hz. These first two levels of triggering rely mainly on hardware and firmware. The third and final level of the trigger, with access to all the event information, uses software algorithms and a computing farm and reduces the output rate to ≈ 50 Hz, which is written to tape.

This analysis uses reconstructed dilepton (ee , $\mu\mu$, $e\mu$) and dijet events collected at D0 from 2002-2004 for both signal and background studies. Integrated luminosities for the eee , $ee\mu$, $\mu\mu e$ and $\mu\mu\mu$ final states are 320 pb^{-1} , 292 pb^{-1} , 285 pb^{-1} , and 289 pb^{-1} , respectively, with a common uncertainty of 6.5% [10]. With three high- p_T charged leptons in the candidates, the overall trigger efficiency for WZ signal is 99.9%.

Electrons are identified by their distinctive pattern of energy deposition in the calorimeter and by the presence of a track in the central tracker that extrapolates from the interaction vertex to a cluster of hits in the calorimeter. Electrons measured in the CC (EC) must have $|\eta| < 1.1$ ($1.5 < |\eta| < 2.5$). The transverse energy of an electron must satisfy $E_T > 15.0$ GeV. An acceptable electron must have an electromagnetic-energy (EM) fraction, $f_{EM} > 0.9$, where f_{EM} is a ratio of energy found in the EM cells of the calorimeter to the total energy of a shower. The isolation $\mathcal{I} = E_{TOT}(0.4)/E_{EM}(0.2) - 1$, must satisfy $\mathcal{I} < 0.15$, where $E_{TOT(EM)}(\Delta\mathcal{R})$ is the total (electromagnetic) energy contained in a cone of angular width $\Delta\mathcal{R} = \sqrt{(\Delta\phi)^2 + (\Delta\eta)^2}$, with ϕ the azimuthal angle, and $\Delta\eta = \Delta\phi = 0$ corresponding to the shower direction in the calorimeter. Further shape information is obtained from a covariance matrix based on 7(8) variables for CC (EC) clusters that is used to construct a χ^2 that represents the consistency of a cluster with an electron shower. The χ^2 selection retains $\approx 95\%$ of all true electrons. Finally, a good electron shower must have a matched track in the central tracking system with the ratio of calorimeter energy to spectrometer momentum E/p within expectations.

Muons are reconstructed using information from the muon, scintillation, central tracking, and calorimeter detectors. A muon reconstructed in the toroid system must have a matching central track with $p_T > 15$ GeV/c. Muon isolation requires transverse energies of calorimeter cells in an annular ring $0.1 < \Delta\mathcal{R} < 0.4$ around each muon direction to satisfy $\sum_{\text{cells}, i} E_T^i < 2.5$ GeV. In addition, the sum of the transverse momenta of all tracks, excluding the muon, in a cone of $\Delta\mathcal{R} = 0.5$ around the muon track must be < 3.5 GeV/c.

The WZ diboson event selection requires three reconstructed leptons, all of which must originate from a common interaction vertex, that pass electron or muon identification criteria outlined above. To avoid confusion between tracks, the separation between any pair of leptons must be $\Delta\mathcal{R} > 0.2$. Figure 2 compares the dilepton invariant mass and \cancel{E}_T distributions expected for WZ events to those from $Z + \text{jets}$, where the Z boson and the W boson have decayed in the muon channel. To select Z bosons and further suppress backgrounds, the invariant mass of a like-flavor lepton pair must fall within $71 \text{ GeV}/c^2$ to $111 \text{ GeV}/c^2$ for e^+e^- events, and $51 \text{ GeV}/c^2$ to $131 \text{ GeV}/c^2$ for $\mu^+\mu^-$ events, with the mass windows set by resolution. For the eee and $\mu\mu\mu$ channels, the lepton pair with invariant mass closest to the Z mass is chosen as the Z candidate. The \cancel{E}_T is required to be greater than 20 GeV, consistent with a W boson decay. The transverse mass is calculated from the p_T of the un-paired third lepton and the \cancel{E}_T . Finally, to reject background from $t\bar{t}$ events, the vector sum of the transverse energies in all calorimeter cells, excluding the leptons, must be less than 50 GeV.

The event selection requirements described above were chosen with the goal of preserving the expected signal while at the same time, reducing the background and its associated uncertainty. signal and background events, respectively.

N_s is calculated using the SM predicted WZ cross section; and N_s and N_b depend on selection. Applying all selection requirements leaves one eee and two $\mu\mu\mu$ candidates. Table I summarizes the event information.

TABLE I: Properties of the three WZ candidates. Units for p_i ($i = x, y, z$), E , $m_{\ell\ell}$, and m_T are GeV, where $m_{\ell\ell}$ is the invariant mass of the two leptons closest to the Z mass, \cancel{E}_T is the missing transverse energy, $\phi(\cancel{E}_T)$ is the azimuthal angle of the \cancel{E}_T vector, and m_T is the transverse mass computed from the unpaired charged lepton and the \cancel{E}_T vectors in the x, y plane [11].

Final State	ℓ_1 p_x, p_y p_z, E	ℓ_2 p_x, p_y p_z, E	$m_{\ell\ell}$	\cancel{E}_T $\phi(\cancel{E}_T)$	ℓ_3 p_x, p_y p_z, E	m_T
eee	-47.3,-25.9	13.3,37.6	91.9	30.6	45.3,-32.1	72.3
	291.8,296.7	110.8,117.8		3.364	-16.5,57.9	
$\mu\mu\mu$	24.5,11.6	-38.7,-12.4	82.1	31.2	-19.3,-16.7	56.4
	29.7,40.2	-17.1, 44.1		0.665	101.4,104.6	
$\mu\mu\mu$	-15.1,19.9	20.2,-42.5	68.5	43.1	-21.9,-5.9	62.5
	24.4,35.0	57.1,74.0		0.338	-16.4, 28	

Acceptances include geometric and kinematic effects and are obtained using Monte Carlo samples produced with the PYTHIA event generator [12] and simulated via the GEANT-based [13] $D\bar{O}$ detector-simulation program. Acceptances are calculated by counting the number of events that pass all selection criteria, except the lepton identification and the track-matching requirements. The results are 0.283 ± 0.009 , 0.279 ± 0.008 , 0.287 ± 0.009 and 0.294 ± 0.008 for eee , $ee\mu$, $\mu\mu e$ and $\mu\mu\mu$ final states, respectively.

Lepton-identification and track-matching efficiencies are estimated using $D\bar{O}$ data samples of $Z \rightarrow e^+e^-$ and $Z \rightarrow \mu^+\mu^-$ events. The $Z \rightarrow \ell^+\ell^-$ invariant mass distribution is fitted with a signal function consisting of a Breit-Wigner convoluted with a Gaussian, and an exponential to describe the background. The area under the signal function returned by the fit defines the number of Z boson events. One of the leptons from the Z decay is required to pass all lepton selection requirements. Identification and track-matching efficiencies are then determined by comparing the number of fitted Z boson events obtained by applying selection criteria to the second lepton with the number obtained with no selection criteria applied. Average identification efficiencies are 0.929 ± 0.013 and 0.965 ± 0.008 for CC and EC electrons, respectively, and 0.940 ± 0.002 for muons. Track-matching efficiencies are 0.817 ± 0.002 for CC electrons, 0.674 ± 0.006 for EC electrons, and 0.950 ± 0.002 for muons. Both identification efficiencies and track-matching efficiencies are further determined as functions of p_T and η , and these dependencies are applied to each lepton in WZ MC events used for selection efficiency calculations. The overall WZ acceptance times detection efficiencies are $(10.3 \pm 1.5)\%$, $(11.7 \pm 0.8)\%$, $(13.9 \pm 1.3)\%$ and $(16.3 \pm 1.8)\%$ for eee , $ee\mu$, $\mu\mu e$ and $\mu\mu\mu$, respectively.

From the SM prediction for σ_{WZ} and the leptonic branching fractions of the W and Z bosons [14], we expect 0.44 ± 0.07 , 0.45 ± 0.04 , 0.53 ± 0.06 , 0.62 ± 0.08 events for the eee , $ee\mu$, $\mu\mu e$, and $\mu\mu\mu$ final states, respectively. Quoted uncertainties include statistical and systematic contributions, as well as the common 6.5% luminosity uncertainty.

No known SM processes other than WZ production produces events with three isolated leptons with large transverse momentum in the final state. The main background to this channel comes from $Z + X$ ($X = \text{jets}, \gamma$ and Z) events. In $Z + \text{jets}$ events, the jets may mimic leptons in the detector. This background is estimated from $D\bar{O}$ data as follows. Events are selected using the same criteria as for the WZ sample, except that the requirement for the third lepton is dropped. The resulting sample includes $ee + \text{jets}$, $\mu\mu + \text{jets}$ and $e\mu + \text{jets}$. Probabilities for jets to mimic electrons or muons are then determined using $D\bar{O}$ dijet data. The jets are reconstructed and ordered in E_T so that, e.g., the E_T of jet $j1$ (E_T^{j1}) is larger than that of jet $j2$ (E_T^{j2}). The second jet then provides an unbiased sample of jets suitable for lepton misidentification studies. The fraction of second jets that satisfy the criteria $|\phi_{j1} - \phi_{j2} - \pi| < 0.3$ and $E_T^{j2} > E_T^{j1}/3$ and pass the lepton selection criteria provides the probability for a jet to be misidentified as a lepton. These misidentification probabilities are calculated as a function of jet E_T and of jet η . Applying the misidentification probabilities to jets in the dilepton + jets data yields the total background from multijets, estimated to be 0.35 ± 0.02 events. A second kind of background is $Z + \gamma$ events, where a γ converted to electrons or randomly matches a charged track in the detector causing it to be misidentified as an electron. Such backgrounds contributes to both $\mu\mu e$ and eee final states. We estimated the $Z + \gamma$ background using events with two EM objects. We found that the probability for a photon to mimic an electron is about 2%. We applied that probability to the observed $Z + \gamma$ data sample that corresponds to this data. After further applying the \cancel{E}_T cut, we estimated the $Z + \gamma$ background to be 0.145 ± 0.020 . Backgrounds from ZZ and $t\bar{t}$ production are found by Monte Carlo method to be 0.20 ± 0.07 and 0.01 ± 0.01 events, respectively. Other sources of background are found to be negligible. The total background is estimated to be 0.71 ± 0.08 events.

The 2.04 ± 0.13 expected WZ events combined with the 0.71 ± 0.08 estimated background events are consistent with the three candidate events found in the data. Table II summarizes results for the four trilepton channels. The

probability for a background of 0.71 events to fluctuate to three or more candidates is 3.5%. Following the method described in Refs. [14] and [15], we use a maximum likelihood technique to obtain $\sigma_{WZ} = 4.5_{-2.6}^{+3.8}$ pb and calculate the 95% C.L. upper limit $\sigma_{WZ} < 13.3$ pb for $\sqrt{s} = 1.96$ TeV. The likelihood function is calculated separately for each final state and then combined, with luminosities for the four trilepton states ranging from 285–320 pb^{-1} .

TABLE II: The number of candidate events, the overall efficiency, the expected number signal events according to the SM and the estimated number of background events in each decay channel.

Decay Channel	Number of Candidates	Overall Efficiency	Expected Signal	Estimated Background
eee	1	0.103 ± 0.015	0.44 ± 0.07	0.155 ± 0.043
$ee\mu$	0	0.117 ± 0.008	0.45 ± 0.04	0.073 ± 0.029
$\mu\mu e$	0	0.139 ± 0.013	0.53 ± 0.06	0.349 ± 0.034
$\mu\mu\mu$	2	0.163 ± 0.018	0.62 ± 0.08	0.132 ± 0.053
Total	3	-	2.04 ± 0.13	0.71 ± 0.08

With σ_{WZ} consistent with SM expectations, we go on to extract WWZ couplings. Two grids are constructed, one in the $\lambda_Z, \Delta g_1^Z$ ($\equiv g_1^Z - 1$) plane (with $\kappa_Z - 1 \equiv \Delta\kappa_Z = 0$), and the other in the $\lambda_Z, \Delta\kappa_Z$ plane (with $\Delta g_1^Z = 0$). Simulated $WZ \rightarrow$ trilepton events [16] are then generated at each grid point, processed with the $D\mathcal{O}$ parametrized detector simulation program, and analyzed using the same selection criteria applied to the data as described above to determine the predicted signal at each grid point. These predictions are used with the background estimated above and the three observed trilepton candidates in the data to construct a likelihood function L . Analyses of contours of L about its maximum value then permit limits to be set on $\lambda_Z, \Delta g_1^Z$ and $\Delta\kappa_Z$, both individually and in pairs. Unitarity requires the anomalous couplings to be multiplied by a form factor containing a scale Λ [17]. Table III lists one-dimensional 95% C.L. limits on $\lambda_Z, \Delta g_1^Z$ and $\Delta\kappa_Z$ with $\Lambda = 1$ TeV or $\Lambda = 1.5$ TeV; and Fig. 3 shows two-dimensional 95% C.L. contour limits for $\Lambda = 1$ TeV. The value of the form factor was chosen such that the coupling limit was less than the unitarity limit [17]. We are not able to set the $\Delta\kappa$ limit for $\Lambda = 1.5$ TeV since the experimental limit exceeds the unitarity limit.

TABLE III: One-dimensional 95% C.L. intervals on $\lambda_Z, \Delta g_1^Z$, and $\Delta\kappa_Z$.

$\Lambda = 1$ TeV	$\Lambda = 1.5$ TeV
$-0.53 < \lambda_Z < 0.56$	$-0.48 < \lambda_Z < 0.48$
$-0.57 < \Delta g_1^Z < 0.76$	$-0.49 < \Delta g_1^Z < 0.66$
$-2.0 < \Delta\kappa_Z < 2.4$	-

In summary, we searched for WZ production in $p\bar{p}$ collisions at $\sqrt{s} = 1.96$ TeV. In a sample of 285 to 320 pb^{-1} , three candidate events were found with an expected background of 0.71 ± 0.08 events. The 95% C.L. upper limit for the WZ cross section is 13.3 pb. Interpreted as a WZ signal, we find $\sigma_{WZ} = 4.5_{-2.6}^{+3.8}$ pb and provide the first measurement of the WZ production cross section in hadron colliders. We used the result to obtain the tightest available limits on anomalous WWZ couplings derived from a WZ final state. Furthermore, they are the most restrictive model-independent WWZ anomalous coupling limits available and represent an improvement by a factor of three over the previous best results.

-
- [1] K. Hagiwara, R.D. Peccei, D. Zeppenfeld, and K. Hikasa, Nucl. Phys. **B282**, 253 (1987).
[2] $D\mathcal{O}$ Collaboration, B. Abbott *et al.*, Phys. Rev. D **60** 072002 (1999). This paper contains a detailed description of the first $WZ \rightarrow$ trileptons search with anomalous WWZ coupling limits and a search for non-standard model $WW + WZ \rightarrow \ell\nu$ jet jet production with limits on anomalous $WW\gamma$ and WWZ couplings.
[3] LEP Electroweak Working Group, D. Abbaneo *et al.*, hep-ex/0412015, and references therein.
[4] CDF Collaboration, F. Abe *et al.*, Phys. Rev. Lett. **75**, 1017 (1995). This paper contains a description of the first search for non-standard model $WW + WZ \rightarrow \ell\nu$ jet jet production with limits on anomalous $WW\gamma$ and WWZ couplings.

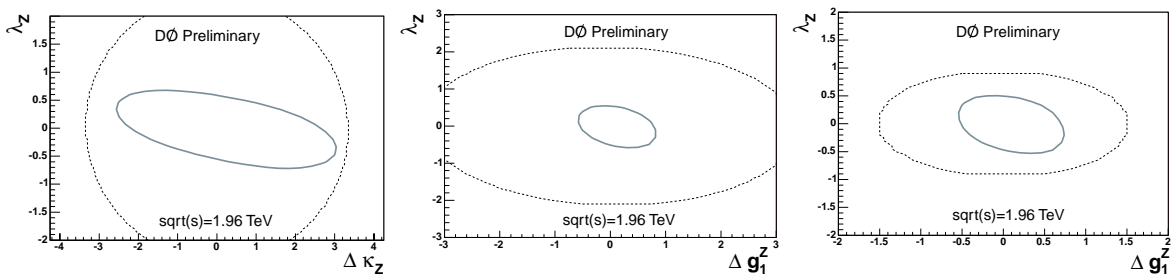


FIG. 3: Two-dimensional coupling limits at 95% C.L. The uppermost figures are λ_Z versus $\Delta\kappa_Z$ and λ_Z versus Δg_1^Z at $\Lambda = 1$ TeV. The lower figure is λ_Z versus Δg_1^Z at $\Lambda = 1.5$ TeV. The inner solid contours are the experimental 95% C.L. limits and the outer dashed contours show the unitarity limits for the respective Λ .

- [5] K. Hagiwara, S. Ishihara, R. Szalapski, and D. Zeppenfeld, Phys. Rev. D **48**, 2182 (1993). They parameterize WWZ couplings in terms of the $WW\gamma$ couplings: $\Delta\kappa_Z = \Delta\kappa_\gamma(1 - \tan^2\theta_w)/2$, $\Delta g_1^Z = \Delta\kappa_\gamma/(2\cos^2\theta_w)$ and $\lambda_Z = \lambda_\gamma$.
- [6] J. M. Campbell and R. K. Ellis, Phys. Rev. D **60**, 113006 (1999); private communication with authors.
- [7] CDF Collaboration, D. Acosta *et al.*, submitted to Phys. Rev. D; hep-ex/0501021.
- [8] S. Abachi *et al.*, Nucl. Instrum. Methods Phys. Res. A **338**, 185 (1994).
- [9] V. Abazov, *et al.*, in preparation for submission to Nucl. Instrum. Methods Phys. Res. A; and T. LeCompte and H. T. Diehl, Ann. Rev. Nucl. Part. Sci. **50**, 71 (2000).
- [10] T. Edwards *et al.*, FERMILAB-TM-2278-E (2004).
- [11] We use a right-handed coordinate system with \hat{z} being the direction traveled by the incoming proton beam and \hat{y} being upwards.
- [12] T. Sjöstrand *et al.*, Computer Physics Commun. **135**, 238 (2001).
- [13] R. Brun *et al.*, CERN-DD-78-2-REV (unpublished).
- [14] Particle Data Group, K. Hagiwara *et al.*, Phys. Rev. D **66**, 010001 (2002).
- [15] G.J. Feldman and R.D. Cousins, Phys. Rev. D **57**, 3873 (1998).
- [16] K. Hagiwara, J. Woodside, and D. Zeppenfeld, Phys. Rev. D **41**, 2113 (1990).
- [17] U. Baur, hep-ph/9510265 and UB-HET-95-04 (unpublished).